Synthesis, characterization, and high potential of 3D metal–organic framework (MOF) nanoparticles for curing with epoxy

Maryam Jouyandeh[a,b], Farimah Tikhani[c], Meisam Shabanian[d], Farnaz Movahedi[d], Shahab Moghari[c], Vahideh Akbari[e], Xavier Gabrion[f], Pascal Laheurte[g], Henri Vahabi[a,b,*], Mohammad Reza Saeb[e,*]

[a]*Université de Lorraine, CentraleSupélec, LMOPS, F-57000 Metz, France*

[b]*Laboratoire Matériaux Optiques, Photoniques et Systèmes, CentraleSupélec, Université Paris-Saclay, 57070, Metz, France*

[c]*School of Chemical Engineering, College of Engineering, University of Tehran, Tehran 11155-4563, Iran*

[d]*Faculty of Chemistry and Petrochemical Engineering, Standard Research Institute (SRI), P.O. Box 31745-139, Karaj, Iran*

[e]*Department of Resin and Additives, Institute for Color Science and Technology, P.O. Box: 16765-654, Tehran, Iran*

[f]*Univ. Bourgogne Franche-Comté, FEMTO-ST Institute, UFC/CNRS/ENSMM/UTBM, Department of Applied Mechanics, F-25000, Besançon, France*

[g]*Universite de Lorraine, Laboratoire LEM3 UMR 7239, Metz, F-57045, France*

g

To whom correspondence should be addressed:

*H. Vahabi, PhD; Tel.: + 33(0)3 87 93 91 86; Fax: +33 (0)3 87 93 91 01; E-mail: henri.vahabi@univ-lorraine.fr

* M.R. Saeb, PhD; Tel.: + 98 (0) 21 229 56 209 ; Fax: + 98 (0) 21 229 47 537; E-mail: mrsaeb2008@gmail.com

Abstract

In this study, the potential of microporous 3D metal–organic framework (MOF) for curing epoxy resin has been discussed. First, MIL-101 (Cr), a chromium based MOF, was synthesized under hydrothermal condition and then characterized by using Fourier transform infrared (FTIR) spectroscopy, X-ray diffraction (XRD) and thermogravimetric (TGA) measurements. Epoxy nanocomposites containing 0.1, 0.3 and 0.5 wt.% of MOF nanocrystals were subsequently prepared and their curability was studied in terms of the universal dimensionless *Cure Index* (*CI*) criterion under nonisothermal differential scanning calorimetry (DSC). Based on calculations made on the basis of the *CI*, epoxy nanocomposites containing 0.1, 0.3, and 0.5 wt.% of MOF were labeled *Good* and *Excellent* thanks to an enhanced chemical interaction between MOF and epoxy matrix, where the heat of cure in the system was surprisingly even higher than that of the neat epoxy. It was demonstrated that introduction of MOF into epoxy significantly improved the heat release during crosslinking process of epoxy, as indicated by a 63% rise in the enthalpy of cure at MOF loading of 0.1 wt.%. Addition of thermally stable MOF nanomaterials to the epoxy resin improved thermal decomposition resistance of epoxy. Up to 0.3 wt.% loading, the system revealed acceptable thermal stability at elevated temperature featured by more residue remained at the end of test, while sample containing 0.5 wt.% MOF resisted against decomposition at early stages of degradation due to higher thermal stability of MOF with respect to epoxy resin.

Keywords: Epoxy; *Cure Index*; 3D nanoparticles; metal–organic framework (MOF)

1. Introduction

Crosslinking state of thermosetting materials can be governed by several materials and processing parameters [1, 2]. Nanoparticles are commonly applied in such systems to play an important role in cure progress [3-5]. With a focus on performance of epoxy coatings and the fact that all ultimate properties of the coatings are dependent on molecular microstructure and interactions, application of nanomaterials in these multipurpose systems is of great significance [6, 7]. The amount of nanoparticles incorporated in nanocomposites, their morphology and functionalization determine the facility or difficulty of network formation, such that allows for demonstration of structure-properties relationship [8-10]. This can be tracked through thermal analysis including differential scanning calorimetry (DSC) that provides valuable information about thermal history and behavior of system [11, 12]. For instance, in a recent work we showed that application of halloysite nanotubes with different surface chemistry in epoxy resin changes the mechanism of crosslinking through which the curing components react to form a thermoset network [13]. The permeability of nanotubes' lumen into curing agent appeared to be a conclusive factor governing the final cure state. Besides, in another study, it was revealed that introduction of mesoporous nanoparticles to the resin enhances their dispersion and contribution to cure of polymer matrix thanks to their high surface area, impeding more active sites available for crosslinking reaction [14]. With this in mind, the quality of crosslinking between cure moieties has been defined by a dimensionless criterion, named *Cure Index* (*CI*), which is governed by microstructure of components present in the thermoset system [15]. In our previous works, we calculated the *CI* for several systems containing bare and modified nanoparticles applied in epoxy coatings for cure observations [16, 17]. It was concluded that morphology and porosity of nanoparticles are key factors for cure progress to be controlled over [18-20].

Metal-Organic Frameworks (MOFs) are new class of 3D nanostructures, which have had diverse applications in storage [21, 22], separation [23, 24], catalysis [25, 26] and recently in biomedicine [27, 28], due to their porosity and/or guest exchange properties. Generally, linking metal ions or metal oxides by polyatomic organic ligands ends in formation of crystalline MOF. The structural frameworks based on inorganic coordination and their geometries governed by organic ligands' type are shown in **Fig. 1**.

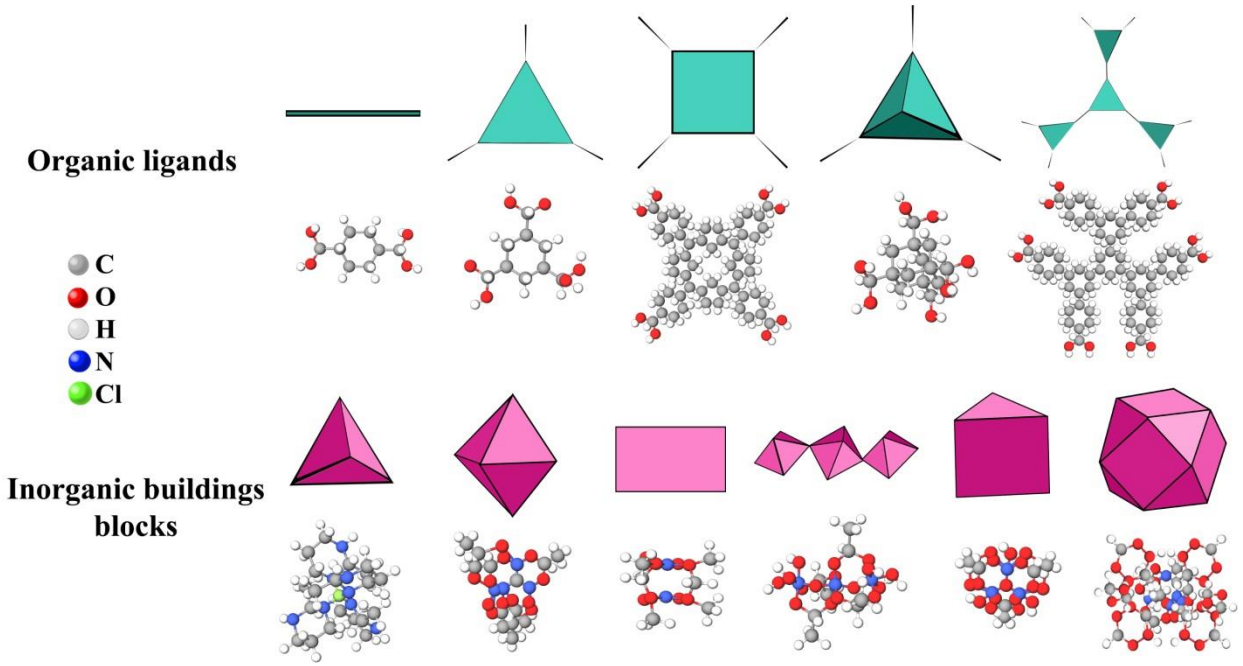

Fig. 1. Classes of inorganic coordination of MOFs and its geometry.

Three prerequisites are mentioned for a material being called as "Metal-Organic Framework": robustness as a result of strong bonding, linking units capable of organic modifications and a well-established geometrical structure or crystallinity. Network connectivity of building units mainly governs the final properties of MOFs [29]. The porous frameworks of unsaturated metal centers in

a certain space result in regioselectivity or shape-/size-selectivity towards guest molecules. Typically, MOF nanomaterials cannot maintain their integrity and functionality in harsh conditions and their stability issues limit their performance. Consequently, studies on the stability of MOFs revealed that strong coordination bonds as well as steric hindrance would help the metal nodes survive the attack of chemical agents and improve their stability. Introduction of high-valent metal ions such as Ti^{4+}, Al^{3+} and Cr^{3+} to MOF structures results in strong coordination bonds inducing high stability in aqueous, acidic and basic conditions [30-32]. Diversity of functionalities in structure of linkers has led to development of new MOFs in recent years [33]. The common ligands that have been involved in MOFs are bipyridyl and carboxylate-based molecules [34]. Among all of the known MOF nanocrystals, MIL-101(Cr) is recognized as a highly stable 3D nanomaterial with Lewis acid sites with chemical structure that can be seen in **Fig. 2**. Removal of water as guest molecules leaves behind the chromium atom accessible for potential reactants which can diffuse into the pore windows [35-37]. Due to the presence of highly inert and strong metal-oxygen (Cr-O) bonds, it is reported that Cr-MOFs show an excellent stability in water, acids and bases [32].

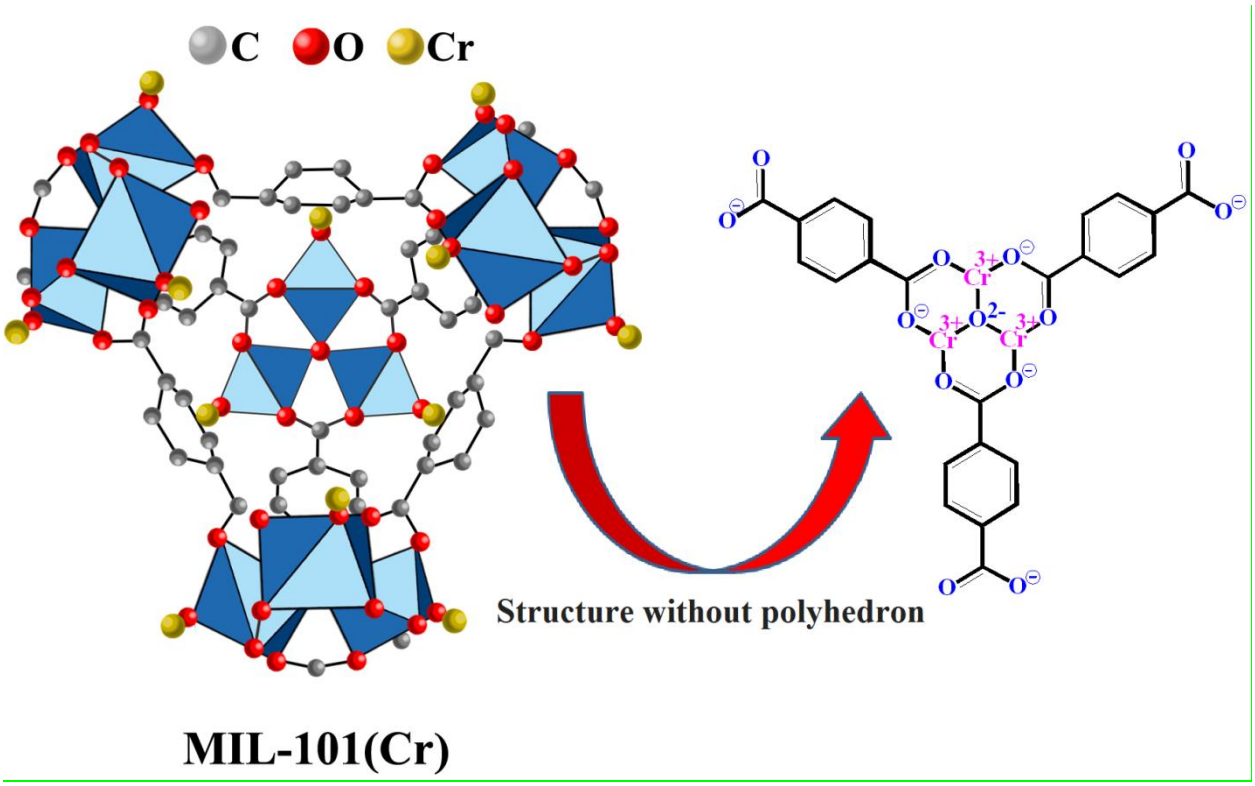

Fig. 2. Chemical structure of MIL-101(Cr) MOF nanocrystals

The general approach for synthesizing these 3D frameworks have been solvothermal method, which is dependent on application of organic solvents in high temperatures [38]. Harmfulness of this expensive method has led scientist to think of a safer synthesis root for different metal frameworks. Qian et al. [39] have applied a hydrothermal method for preparing zeolitic imidazolate frameworks (ZIF) taking place in an aqueous solution and at room temperature. They believe that this method can be extended to synthesize other MOF nanocrystals as well. Besides, the compatibility of MOFs with polymeric systems, as well as their structural diversity, have translated these nanomaterials to strong candidates for nanotechnology applications in order to fulfill various tasks and obtain a multifunctional material [40]. Practical interfacial interactions between matrix polymer chains and components of hybrid MOFs are expected to be achieved due

to high surface area of MOFs. The ligand component makes these nanomaterials more compatible with organic polymers in comparison to other nanomaterials that are in fond of molecular design and interactions. Moreover, concerning nanoparticle dispersion impediment, surface modification is considered as a constructive treatment.

A promising application for MOF is to use them as modifier of epoxy resin to reduce the dielectric constant and enhance mechanical properties [41]. The epoxy/MOF nanocomposites not only combine the high thermal-stability of MOFs and robustness of resin, but also largely overcome the brittleness and limited mechanical strength of the epoxy resin [42, 43]. There are many reports on application of MOFs in epoxy coatings for various purposes. From a mechanical point of view, introduction of 0.1-0.7 wt.% of a kind of MOF nanoparticle to epoxy resin has enhanced fracture toughness and impact strength by 236% and 68%, respectively [44]. Additionally, adsorption and catalytic effect of phosphorus-containing Co-based MOFs in epoxy resin appeared to suppress smoke and toxic compounds release and to improve fire safety of this polymer, which is characterized through heat release reduction [45]. Thanks to low toxicity of MOFs and their massive porosity, they have been good candidates for corrosion inhibition applications. Wang et al. reported dopamine modified MOF, which could significantly improve water and corrosion resistance of waterborne epoxy coatings [46]. Application of hydrothermally synthesized UiO-66 MOFs as a reinforcement of epoxy resin resulted in an interpenetrated composite structure with improved toughness [42]. All these ameliorations rely on high porosity of MOFs, strong interactions and perfect load transfer between nanoparticle and matrix.

In this study, mesostructured MIL-101(Cr) MOF nanocrystals were synthesized through a hydrothermal method. The produced nanocrystals were validated by optical analyses such as Fourier-transform infrared spectroscopy (FTIR) and X-ray diffraction (XRD). Afterwards, the

resulted MOFs were introduced to epoxy resin in three different concentrations of 0.1, 0.3 and 0.5 wt.% to evaluate their contribution to epoxy curing. The cure behavior of system in the presence of nanocrystals was tracked by nonisothermal differential scanning calorimetry (DSC) measuring the enthalpy of cure reaction caused by epoxy ring opening mechanism. State of cure for all the samples has been visualized by the versatile *CI* at distinct heating rates (5, 10, 15 and 20 ºC min^{-1}). Finally, thermal stability of the prepared nanocomposites was evaluated by thermogravimetric analysis (TGA) and compared to blank epoxy.

2. Experimental

2.1. Materials

Epoxy resin RenLam© CY 219 with viscosity of 10000-12000 mPas and density of 1.1 g/cm^3 at 25 °C was purchased from Huntsman. RenLam© HY 5161 was provided by Huntsman and employed as crosslinking agent. The chromium (III) nitrate nonahydrate ($Cr(NO_3)_3.9H_2O$), terephthalic acid, sodium hydroxide and were purchased from Sigma-Aldrich. N,N-dimethylformamide (DMF), methanol and ethanol were purchased from Merck (Germany) and used as received.

2.2. Preparation of MIL-101(Cr)

MIL-101 (Cr) was prepared by a hydrothermal method [47]. In this regard, equimolar amounts of $Cr(NO_3)_3.9H_2O$ (2.0 g, 5 mmol) and terephthalic acid (0.83 g, 5mmol) were added into deionized water (20 mL). The mixture sonicated for 30 minutes, in which resulted to a dark blue-colored suspension, then transferred to a 100 mL Teflon-lined stainless steel autoclave and kept in an oven at 218 °C for 18 h. After natural cooling, the suspension was centrifuged at 10000 rpm for 10 min, repeatedly washed with water. Then the MOF solids were stirred in DMF (20 mL) for 30 min and maintained at 70 °C overnight. The obtained green powders were separated by centrifugation, washed with methanol several times, then vacuum dried at room temperature for two days.

2.3. Preparation of epoxy/MOF nanocomposites

Three epoxy nanocomposite coatings comprising 0.1, 0.3 and 0.5 wt.% pristine MOF were prepared. The nanoparticles were dispersed in epoxy resin containing 5 ml of DMF under sonication using UP200Ht (hielscher) sonicator with amplitude of ultrasound wave of 50% and duty cycle of 50% for 15 min. The resulting nanocomposite was then degassed at 80 °C. Lastly, stoichiometric amount of curing agent (epoxy:hardener=100:50) was thoroughly mixed with neat epoxy and its nanocomposites.

2.4. Characterization methods

2.4.1. Fourier-transform infrared spectroscopy (FTIR)

FTIR analysis (Spectrum one, PerkinElmer Inc., Boston, MA) across the wavenumber of 400-4000 cm^{-1} with spectral resolution of 4 cm^{-1} was collected using a KBr pellet in a transmission mode for MOF and MOF-N.

2.4.2. X-ray diffraction (XRD)

Wide angle XRD analysis was performed by using a diffractometer, Rigaku-MiniflexII (Japan) to evaluate the structure and surface modification of MOFs. Samples were packed into the cavity of a glass sample holder with a depth of 1 mm and leveled to obtain a flat surface. The diffractograms of the samples were scanned in 2θ values in the range of 2° to 30° using CuKα (λ=1.5418) radiation at voltage of 30 kV and current of 15 mA.

2.4.3. Nonisothermal differential scanning calorimetry (DSC)

Cure characterization of the neat epoxy and its nanocomposite containing 0.1, 0.3 and 0.5 wt.% of pristine and modified MOF were studied on a NETZSCH 200F3 Maia Differential Scanning Calorimeter (Netherland) and a 409 PC Luxx Simultaneous Thermal Analyzer (STA). 15 mg of the samples were mixed with stoichiometric amount of curing agent and placed in aluminum DSC sample holder. Then, the sample was nonisothermally heated at heating rates of 5, 10, 15, and 20 ^{o}C min^{-1} in the temperature range of 20–300 ^{o}C under nitrogen with the flow rate of 50 ml min^{-1}.

2.4.4. Thermogravimetric analysis (TGA)

Thermal stability of epoxy in the presence of different contents of MOF was investigated by Setaram Labsys Evo thermogravimetric analyzer (France). The completely cured samples were placed in a ceramic pan and heated from room temperature up to 800 ^{o}C with a constant nitrogen flow rate of 50 ml.min^{-1} at heating rate of 10 ^{o}C min^{-1}.

3. Results and discussions

3.1. Characterization of Synthesized MOF

3.1.1. FTIR characterization

With the intention of tracking the successful synthesis of MOF nanoparticles, FTIR spectra of MIL-101(Cr) is shown in **Fig.3**. The Cr-O bonding absorption of synthesized MOF appeared at 582 cm^{-1} [48]. C-H vibrations of aromatic rings is obvious at 750 cm^{-1} as a sharp peak. It is worth noting that the distinct peaks at 1394 cm^{-1} and 1627 cm^{-1} are ascribed to vibrational stretching frequencies of O-C-O and C=O bonds, which confirm presence of dicarboxylate within 3D

nanomaterials [49, 50]. The peak at 3380 cm^{-1} is imputed to aromatic O-H stretching in MOF structure.

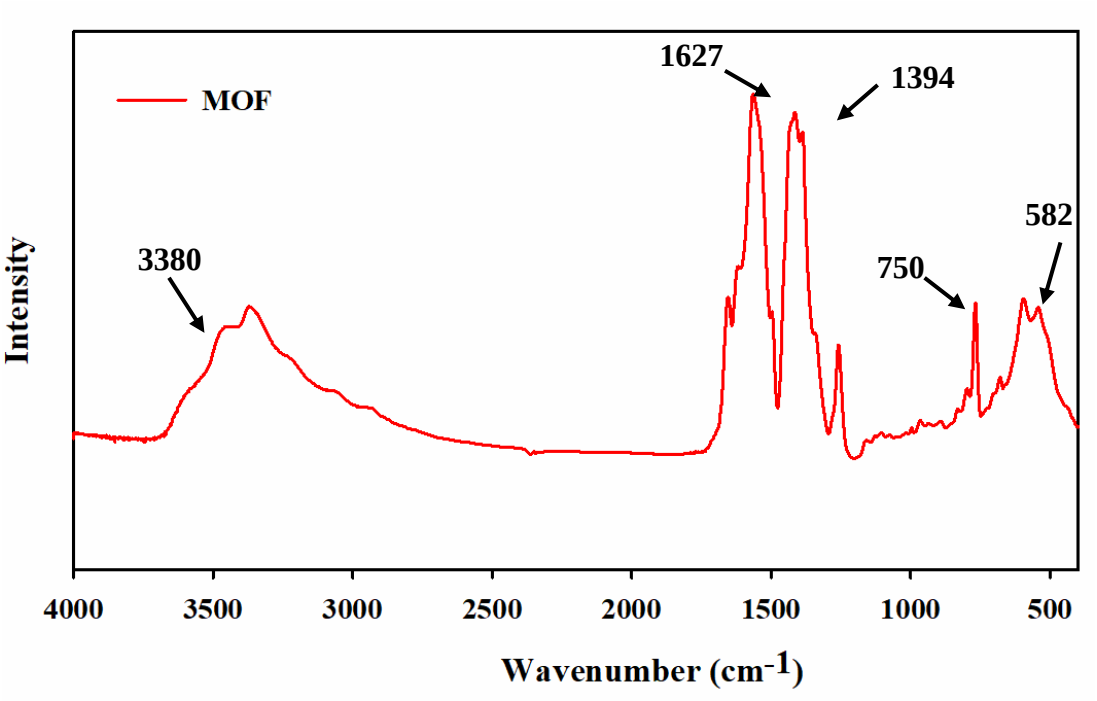

Fig.3: FTIR spectrum of MIL-101(Cr)

3.1.2. XRD characterization

The successful synthesis of chromium derived MIL-101 MOFs was confirmed by XRD studies (**Fig.4**). As can be seen from the XRD pattern the main peaks have the same location with the peaks for standard MIL-101(Cr) [51, 52]. High intensities reveals high crystallinity of product [50] and in lower angles is representative of abundant pores in its structure [53]. It is proposed that in hydrothermal synthesis, fluorine is used as mineralizing agent to achieve a well-crystalized porous MOFs [54]. In absence of fluoride anions as a harmful material, which participates in coordination bonds of trimeric chromium species, observance of problems in crystallinity and existence of

amorphous by-products in final product are possible [55]. This explains the broadening of some of Bragg's reflections in the XRD pattern as a result of poorly crystalline phases. The characteristic reflection planes responsible for diffraction peaks are labeled on **Fig. 4**.

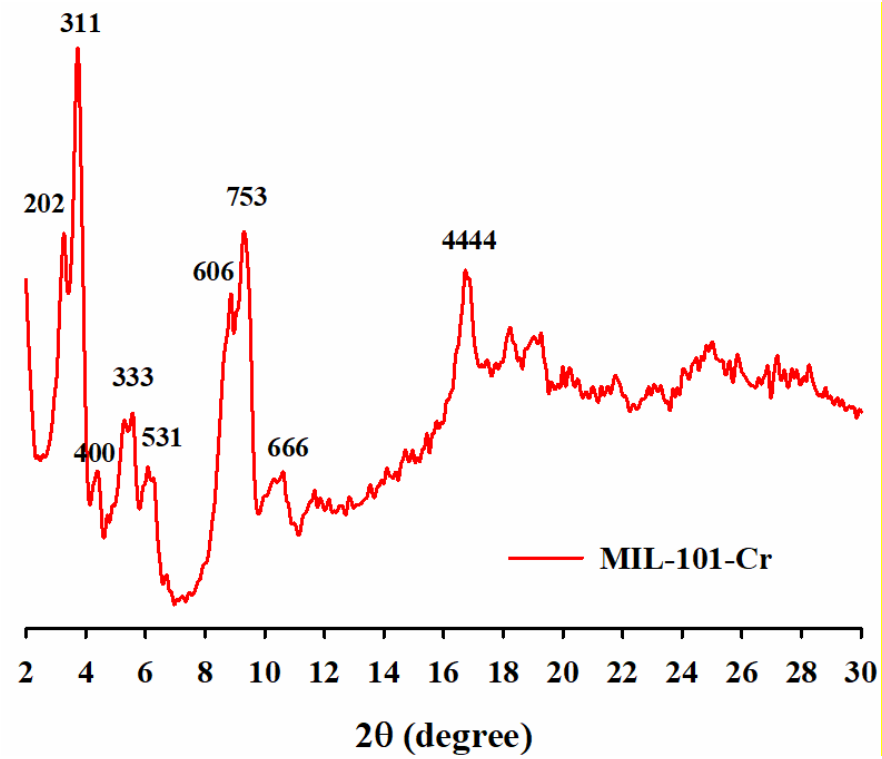

Fig.4: XRD pattern of MIL-101(Cr).

Moreover, the d-spacing calculated by Bragg law (**Eq. (1)**) and *hkl* values based on the diffractogram data of synthesized MIL-101 (Cr) are listed in **Table 1**.

$$d = \frac{\lambda}{\sin\theta} \qquad (1)$$

The resulted values are similar to those reported in literature which confirms the successful synthesis of MIL-101 (Cr) [56].

Table 1. The d-spacings and *hkl* values of XRD powder diagram of MIL-101 (Cr)

2θ (degree)	***d* (A°)**	***h***	***k***	***l***
3.28	26.90474	2	0	2
3.76	23.4711	3	1	1
5.28	16.71718	3	3	3
6.08	14.51923	3	5	1
8.88	9.946382	2	2	8
9.28	9.518537	7	5	3
10.64	8.304738	6	6	6
17.44	5.078959	4	4	16

3.2. Nonisothermal DSC analysis

Nonisothermal DSC analysis was carried out on the blank system and nanocomposites of epoxy containing various amounts of MOF to provide thermograms presented in **Fig. 5**. As it is seen, the measurements were conducted at heating rates (β) of 5, 10, 15 and 20 $^{o}C\ min^{-1}$ which is necessary for qualitative analysis of cure progress with *CI*.

The first inference from unimodal peaks in **Fig. 5** is single step cure kinetics, demonstrating negligibility of side reactions [57, 58]. As observed, epoxy ring opening reaction starts from room temperature for heating rate of 5 $^{o}C\ min^{-1}$ due to the enough time that is given to cure moieties [11, 59].

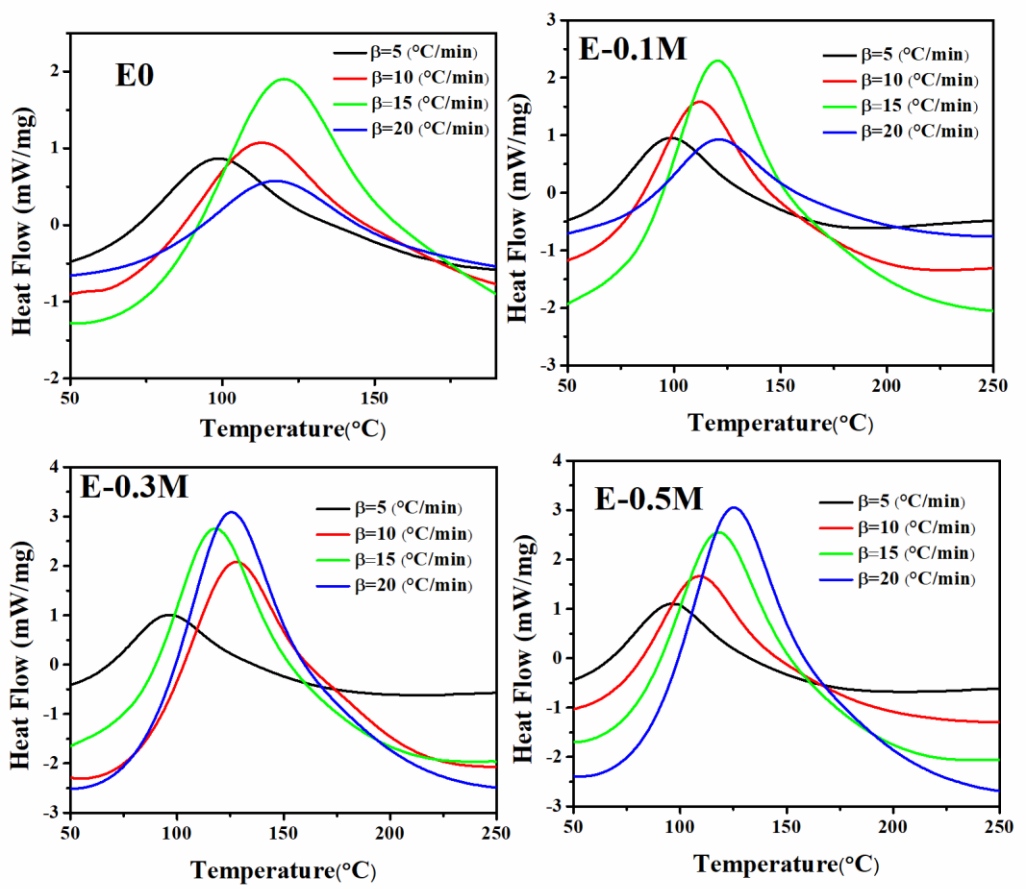

Fig.5: Nonisothermal DSC thermograms of neat epoxy and epoxy nanocomposites containing 0.1, 0.3 and 0.5 wt.% MOF at different heating rates (β) of 5, 10, 15 and 20 °C min^{-1}

Cure characteristics such as onset (T_{onset}), endset (T_{endset}) and peak (T_p) temperatures of curing reaction for neat epoxy and its nanocomposites were extracted from DSC curves and reported in **Table 2**. The curing temperature interval or window $\Delta T = T_{endset} - T_{onset}$ is also listed in **Table 2**. Moreover, the enthalpy of cure (ΔH_∞) which is the heat that released during the curing reaction obtained by calculating the area under exothermic curve of DSC thermograms based on the extrapolated baseline listed in **Table 2**.

All of the qualitative evaluations mentioned above about cure situation of epoxy nanocomposites can be summarized in *Cure Index* (*CI*), a versatile and inclusive criterion that is defined as below [15]:

$$CI = \Delta H^{*} \times \Delta T^{*} \quad (2)$$

Where:

$$\Delta T^{*} = \frac{\Delta T_{C}}{\Delta T_{\mathrm{Re}\,f}} \quad (3)$$

$$\Delta H^{*} = \frac{\Delta H_{C}}{\Delta H_{\mathrm{Re}\,f}} \quad (4)$$

ΔH_C and ΔH_{Ref} are the total heat that is released throughout cross-linking of the thermoset composites and the neat epoxy, respectively. Besides, ΔT_C and ΔT_{Ref} indicate temperature window within which cure is taking place for nanocomposites and the neat epoxy resin, respectively. The values of ΔT^{*}, ΔH^{*} and *CI* are calculated for the prepared epoxy nanocomposites at four heating rates of 5, 10, 15 and 20 °C min^{-1} (**Table 2**). The dimensionless parameters provide the opportunity of cure evaluation without any needed chemistry considerations. It is worth mentioning that the value of *Cure Index* is not what evaluates the cure quality, but the range in which the index appears does so. This makes the *CI* a qualitative criterion despite the fact that it is a number. Inquiring into the **Table 2**, one can find out that ΔH_C is comparatively greater than blank epoxy samples, which is the desirable behavior for cure enhancement. Therefore, in this case, ΔT_C is the decisive parameter to adopt resolutions about cure improvement. If the introduction of nanoparticles tp epoxy system scales down the temperature interval of reaction, it will be considered as an expedient condition to announce the *Excellence* of network formation. Meanwhile, based on *Cure*

Index definition provided in the protocol, observing a boost in both of ΔH_C and ΔT_C parameters in consequence of composition of MOF crystals with polymer is not a distasteful situation and represents *Good* involvement of cure moieties, which results in *CI* exceeding ΔH^* value.

Table 2. Cure characteristics of the prepared epoxy nanocomposites as a function of heating rate

Designation	β(°C min^{-1})	T_p(°C)	ΔT(°C)	ΔH_∞(J/g)	ΔT^*	ΔH^*	*CI*	Quality
E0	5	98.5	182	266.1	n.a.	n.a.	n.a.	n.a.
	10	112.7	160	176.9	n.a.	n.a.	n.a.	n.a.
	15	120.3	199	213.0	n.a.	n.a.	n.a.	n.a.
	20	117.5	157	214.38	n.a.	n.a.	n.a.	n.a.
E-0.1MOF	5	98.5	160	283.1	0.88	1.06	**0.93**	***Excellent***
	10	112.2	181	267.3	1.13	1.51	**1.71**	***Good***
	15	120.5	217	310.0	1.09	1.46	**1.59**	***Good***
	20	120.9	211	348.7	1.34	1.63	**2.18**	***Good***
E-0.3MOF	5	96.1	172	274.4	0.95	1.03	**0.98**	***Excellent***
	10	126.7	192	217.9	1.2	1.23	**1.48**	***Good***
	15	118.0	190	286.2	0.95	1.34	**1.27**	***Excellent***
	20	125.0	210	273.9	1.34	1.28	**1.72**	***Good***
E-0.5MOF	5	95.6	163	289.8	0.90	1.09	**0.98**	***Excellent***
	10	109.4	200	266.2	1.25	1.50	**1.88**	***Good***
	15	118.5	185	265.7	0.93	1.25	**1.16**	***Excellent***
	20	125.7	204	268.7	1.30	1.25	**1.63**	***Good***

n.a. – not applicable (reference measurements)

As the heating rate increases, lack of equilibrium time prevents the reacting molecules from reaching to the active sites, as a result the main peak of cure shifts to higher temperatures [60, 61]. However, the wider temperature window of cure for nanocomposites compared to blank epoxy

unwraps catalytic contribution of nanoparticles in systems. Lower temperature gives dominance to chemical aspect of cure reaction while diffusion governs conversion in higher temperature [62, 63]. Although using 0.1% MOF couldn't change the maximum peak temperature (T_p) significantly compared to blank sample, enhancement of released heat (ΔH_∞) regardless of heating rate shows a promotion in cure state. For the case of E-0.1MOF a significant rise in ΔH_∞ value can be observed from 214 J/g to 349 J/g due to the strong interactions between MOF and the epoxy matrix which can be attributed to the organic–inorganic hybrid nature and high specific surface area of MOFs [64].

Higher loadings of MOF in system not only increase the heat of cure, but also shift T_p for other cases to higher temperatures. MIL-101 (Cr) as hybrid MOF materials of inorganic and organic ligands can take advantage of its organic groups to disperse uniformly through the epoxy matrix even in higher content of 0.3 and 0.5 wt.%. In addition, the high surface area and large pore size of MOF result in noticeable interfacial interactions between the epoxy resin and nanocrystal surface. The strong interface between resin and MOF and the ability of intra-particle diffusion of epoxy within the mesopores of MIL-101 (Cr) with pore diameter of ca. 3 nm led to higher ΔH_∞ values compared to neat epoxy even at higher loading of MOF [65, 66]. It is noteworthy that in our previous work [67], addition of unmodified nanoparticles to epoxy resin mainly exhibited their inhibiting role in crosslinking progress. While here, catalytic effect of MOFs in curing of thermoset resin is prominent, concerning special characteristics of 3D metal-organic frameworks including their compatibility with polymer due to their organic ligands, high surface area and porosity.

The cure state of epoxy/MOF nanocomposites are illustrated schematically in **Fig. 6** which specifies a coordination to each cure state depending on their ΔT^* and ΔH^* values. As it was

mentioned above, the *Excellent* cure condition for an epoxy nanocomposite would happen when the temperature window and released heat of the cure reaction decreases and increases, respectively. This is why the upper left side of the diagram is selected to be green, representing *Excellent* crosslinking. Decreasing the enthalpy of cure in nanocomposites compared to blank sample is an unsatisfactory situation that is colored to red regardless of temperature window changes. Not being in this region would be considered as an improvement in cure behavior. Moreover, concerning results of **Table 2**, one can realize that introduction of organic-metal frameworks to epoxy resin improves cure state of nanocomposites to *Good* and *Excellent* cure compared to blank resin. It is believed that the interactions between components of system are strong enough that even in higher concentrations the *CI* results for heating rate of 5 °C min^{-1} confirms the claim about significant enhancement of cure reaction by appearing to be *Excellent* for all the epoxy/MOF nanocomposites. It is interesting that MOF nanoparticles unconditionally facilitated epoxy ring opening reaction. The reason behind this improvement can be the inner channels of nanocrystals that let the cure moieties diffuse and pass through the nanoparticles and make a dense network. Therefore, none of nanocomposites have been placed in red region which declares proper cure condition provided for the system.

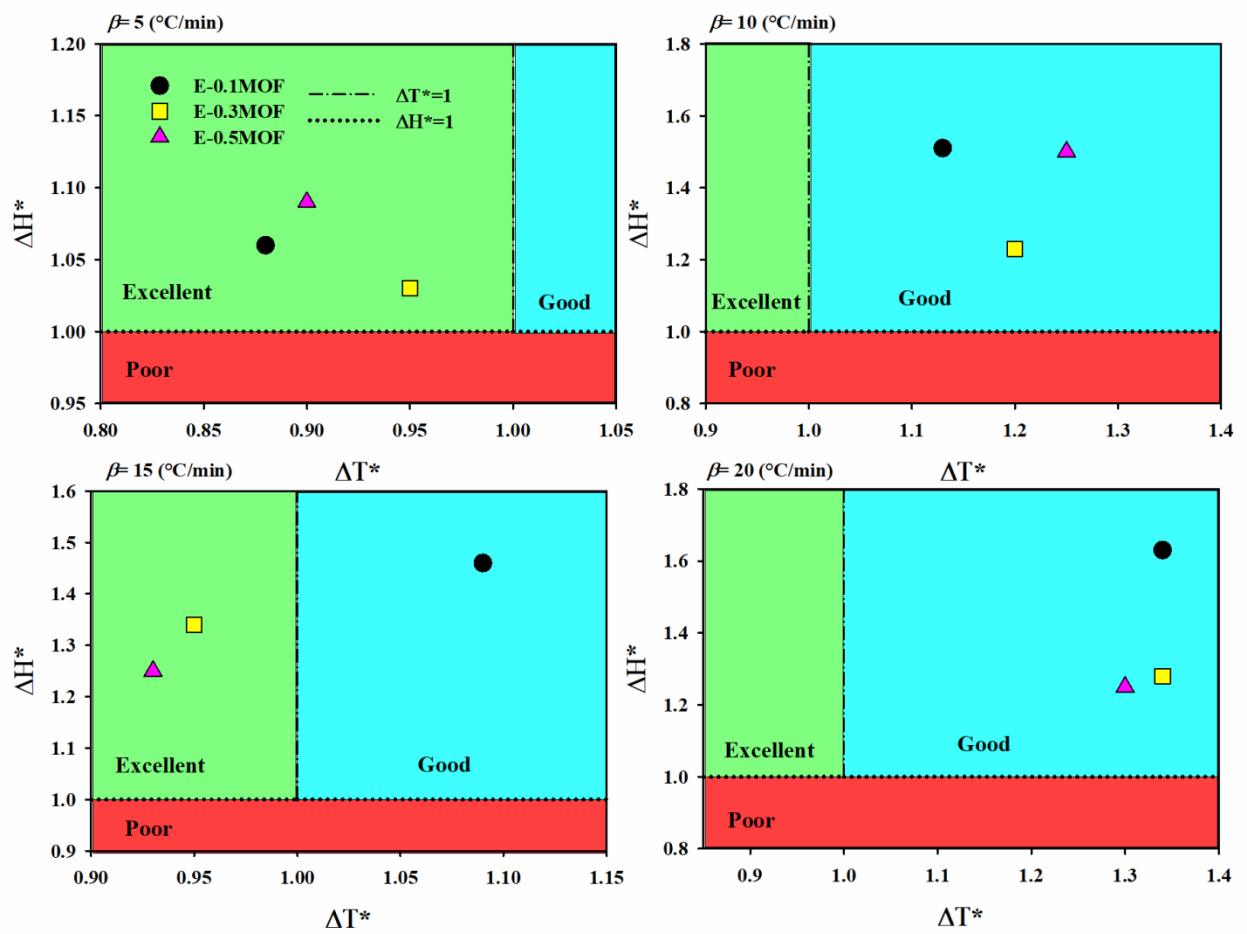

Fig.6. The cure state of epoxy in the presence of 0.1, 0.3 and 0.5 wt.% of MOF nanocrystals at different heating rates which green, blue and red areas show *Excellent*, *Good* and *Poor* cure state in terms of *CI*, respectively.

This fact signifies higher amount of attachment between epoxy groups, hardener and activated chromium atoms in structure of nanocrystals. The pseudo-octahedral coordination sphere around Cr atom in the structure of MIL-101 (Cr) MOF is completed with H_2O molecules, fluorine and OH groups [68]. At high temperature the coordinated water molecules can be easily removed which then let the Cr atoms being available for reacting with epoxide groups due to their Lewis acid effect. In addition, the pore windows of MIL-101 (Cr) are big enough (two internal cages with free

diameters 29 °A and 34 °A [54]) to give access for epoxy pre-polymer diffusing into the pores and reach Lewis acidic sites, exposed to the inner surface and react with them (**Fig. 7**).

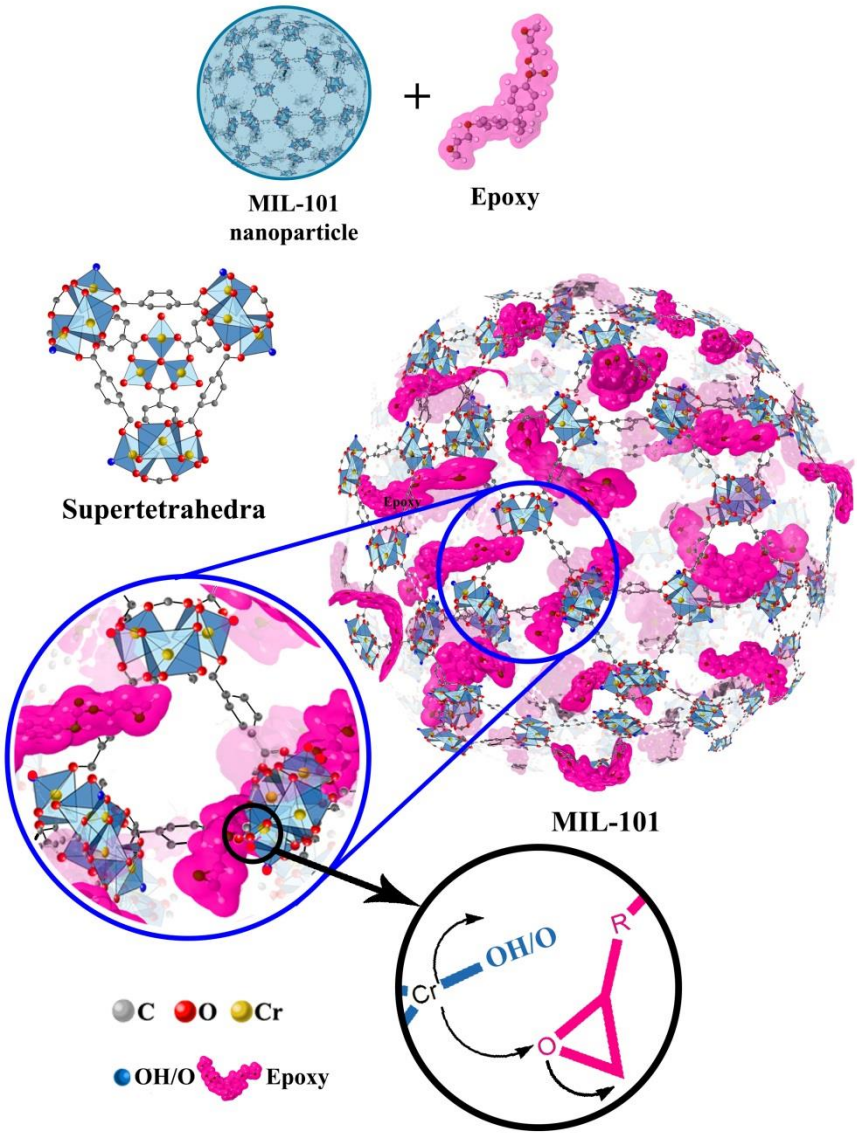

Fig.7. The possible reaction of epoxy with Cr atoms of MIL-101 and diffusing epoxy pre-polymer into the pores of MOF

Nevertheless, since curing agent molecules are smaller than epoxy resin; they have a higher chance for diffusing into the MOF pores. At higher loading of MOF this possibility has become more intense which led to deactivation of a proportion of curing agents and decreased ΔH_{∞} value compared to lower content of MOF. Overall, heating rate is an important parameter in progression of cure reaction [60]. At low heating rates the cuing moieties were supposed to have more time to participate in curing reaction. At high heating rates, there is sufficient amount of kinetic energy per molecule in the system which results in higher vibration of molecules. Another important parameter which can affect cure situation of epoxy nanocomposite is concentration of nanoparticles [13]. By increasing the content of inorganic nanoparticles in epoxy matrix the cure reaction was hindered above a critical level of nanoparticles. In the case of polymer/MOF nanocomposites, the ligand component makes these nanomaterials more compatible with organic polymers in comparison to other nanomaterials. Here because of having MOF with pore volumes of 12,700 °A^3 and 20,600 °A^3 [54], sensitivity of curing to heating rate and concentration was acceptable, so that no *Poor* cured nanocomposite was detected by changing heating rate and concentration.

3.3. Thermal stability analysis

Thermal behavior of neat epoxy and its nanocomposites containing 0.1, 0.3 and 0.5 wt.% of MOF nanopalates were estimated by TGA and shown in **Fig. 8.** As can be observed, a slight weight loss occurred at the first stage of thermal process below 200 ˚C, which is related to evaporation of absorbed water and moisture, solvent and un-reacted materials. The main weight loss of system occurred in the temperature window of 300-400 ˚C due to decomposition of main chain of epoxy [69].

Thermal degradation parameters such as T_5, T_{10}, and T_P which represent decomposition temperature of 5%, 10% and peak weight loss, respectively and char residue at the end of TGA were extracted and reported in **Table 3**.

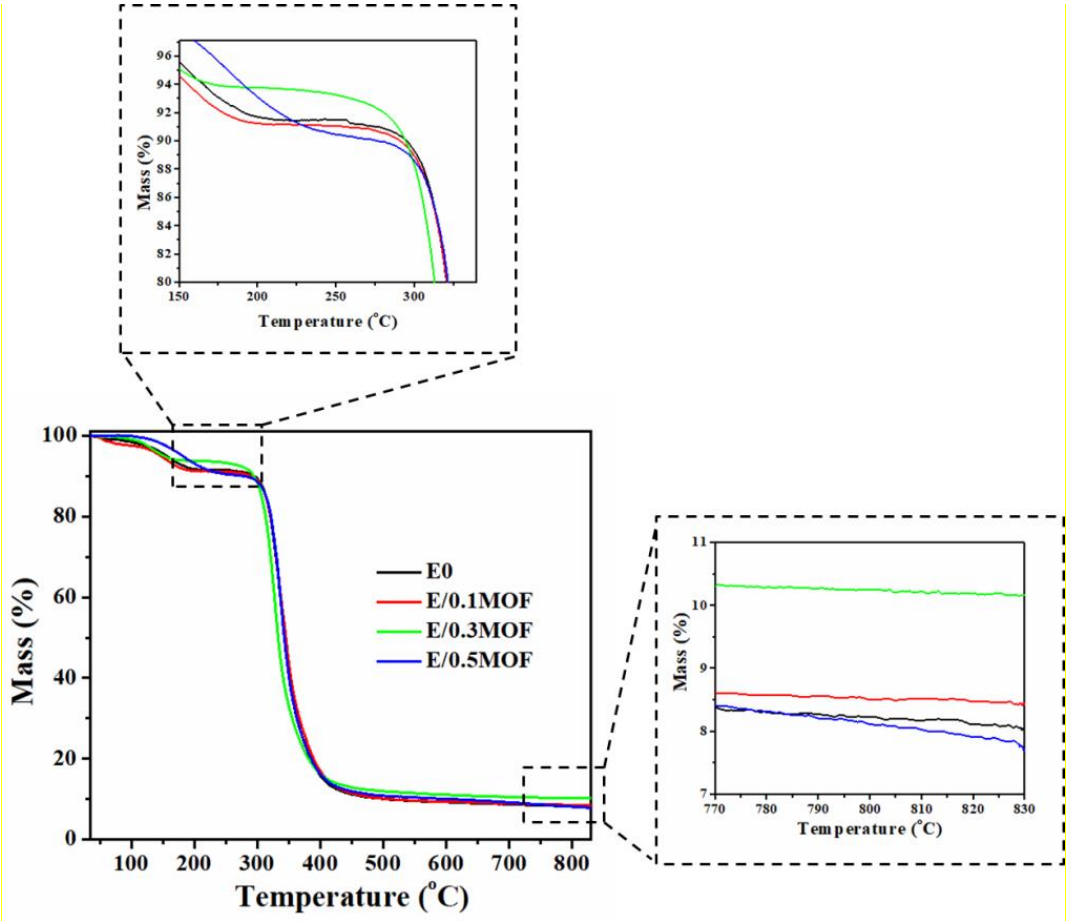

Fig. 8. TGA thermograms of neat epoxy and its nanocomposites at heating rate 10 °C min^{-1}.

As can be observed from **Fig. 8** and **Table 3**, addition of MOF had no significant effect on the epoxy thermal behavior. However, 0.5 wt.% of MOF could improve T_5 about 25 ˚C. On the other hand, although 0.1 and 0.3 wt.% of MOF was not able to improve the thermal stability of epoxy at

early stages of decomposition, its positive effect can be observed at late stage of degradation as higher char amounts. At loadings 0.1 and 0.3 wt.% early stage thermal decomposition was not sensibly governed by MOF addition, although network formation was *Good* based on *CI* (**Table 1**). However, the char residue raised to 8.3 and 10.1 for 0.1 and 0.3 wt.% MOF, respectively. By contrast, at high loading of 0.5 wt.% MOF, early state resistance against decomposition by heat was featured in obviously higher T_5 value, signifying higher thermal stability contributed from more thermally stable MOF particles. On the other hand, residue amount suggests a possible chemical interaction existing at low 0.1 wt. MOF reaching maximum at 0.3 loading level, while the system containing 0.5 wt.% MOF revealed lower thermal resistance at elevated temperatures.

Table 3. Thermal degradation parameters of neat epoxy and its nanocomposites.

Designation	T_5 (°C)	T_{10} (°C)	T_P (°C)	Residue (%)
E0	156.00	295.00	338.00	7.70
E-0.1MOF	145.60	291.10	338.00	8.30
E-0.3MOF	152.00	294.30	328.00	10.10
E-0.5MOF	181.40	277.30	338.00	7.20

Conclusion

MIL-101 (Cr) MOF was synthesized by coordination reaction between $Cr(NO_3)_3.9H_2O$ and terephthalic acid. The chemical and crystalline structure of nanomaterials were compared with references and confirmed through FT-IR and XRD characterizations. The mesoporous nanocrystals were introduced to epoxy resin in different concentrations (0.1, 0.3 and 0.5 wt.% of resin) as an additive which is able to interacts with cure moieties during network formation of thermoset polymer. Noticeable increase in the amount of released heat of cure of epoxy system was the first eye-catching change in comparison to unmodified resin which showed the high

contribution of nanoparticles in cure progress. For instance, the significant rise of 135 J/g in ΔH_∞ value was observed for the case of E-0.1 MOF compared to neat epoxy, representing the cure facilitating nature of nanoparticles even in very low concentration. From *CI* perspective, it was found that at all heating rates *Excellent* and *Good* cure state achieved for all the epoxy/MOF nanocomposites regardless of the MOFs loadings. None of nanocomposites have been placed in red region of *Poor* cure state which declares that MOF nanocrystals facilitate curing reaction of epoxy. This shows the validity and efficiency of illustrative *CI* criterion to judge and characterize thermoset nanocomposites of all kinds. The TGA analysis revealed that thermally-stable MOFs could enhance the thermal performance of epoxy resin which also depended on concentration of nanoparticles. The prepared epoxy nanocomposite of MIL-101 (Cr) can be applicable as smart coatings, using the porous nanoparticles as nanocontainers of corrosion inhibitor.

References

[1] Aliakbari M, Jazani OM, Sohrabian M, Jouyandeh M, Saeb MR. Multi-nationality epoxy adhesives on trial for future nanocomposite developments. Progress in Organic Coatings. 2019;133:376-86.
[2] Bayat S, Moini Jazani O, Molla-Abbasi P, Jouyandeh M, Saeb MR. Thin films of epoxy adhesives containing recycled polymers and graphene oxide nanoflakes for metal/polymer composite interface. Progress in Organic Coatings. 2019:105201.
[3] Karami Z, Jouyandeh M, Ali JA, Ganjali MR, Aghazadeh M, Maadani M, et al. Cure Index for labeling curing potential of epoxy/LDH nanocomposites: A case study on nitrate anion intercalated Ni-Al-LDH. Progress in Organic Coatings. 2019:105228.
[4] Karami Z, Jouyandeh M, Ali JA, Ganjali MR, Aghazadeh M, Maadani M, et al. Development of Mg-Zn-Al-CO3 ternary LDH and its curability in epoxy/amine system. Progress in Organic Coatings. 2019:105264.
[5] Karami Z, Jouyandeh M, Ali JA, Ganjali MR, Aghazadeh M, Maadani M, et al. Cure Index for labeling curing potential of epoxy/LDH nanocomposites: A case study on nitrate anion intercalated Ni-Al-LDH. Progress in Organic Coatings. 2019;136:105228.
[6] Jouyandeh M, Jazani OM, Navarchian AH, Shabanian M, Vahabi H, Saeb MR. Bushy-surface hybrid nanoparticles for developing epoxy superadhesives. Applied Surface Science. 2019;479:1148--60.
[7] Vahabi H, Jouyandeh M, Cochez M, Khalili R, Vagner C, Ferriol M, et al. Short-lasting fire in partially and completely cured epoxy coatings containing expandable graphite and halloysite nanotube additives. Progress in Organic Coatings. 2018;123:160-7.

[8] Jouyandeh M, Zarrintaj P, Ganjali MR, Ali JA, Karimzadeh I, Aghazadeh M, et al. Curing epoxy with electrochemically synthesized GdxFe3-xO4 magnetic nanoparticles. Progress in Organic Coatings. 2019:105245.
[9] Jouyandeh M, Ganjali MR, Ali JA, Aghazadeh M, Karimzadeh I, Formela K, et al. Curing epoxy with ethylenediaminetetraacetic acid (EDTA) surface-functionalized CoxFe3-xO4 magnetic nanoparticles. Progress in Organic Coatings. 2019:105248.
[10] Jouyandeh M, Karami Z, Ali JA, Karimzadeh I, Aghazadeh M, Laoutid F, et al. Curing epoxy with polyethylene glycol (PEG) surface-functionalized NixFe3-xO4magnetic nanoparticles. Progress in Organic Coatings. 2019:105250.
[11] Jouyandeh M, Paran SMR, Jannesari A, Puglia D, Saeb MR. Protocol for nonisothermal cure analysis of thermoset composites. Progress in Organic Coatings. 2019;131:333--9.
[12] Vyazovkin S, Burnham AK, Criado JM, Pérez-Maqueda LA, Popescu C, Sbirrazzuoli N. ICTAC Kinetics Committee recommendations for performing kinetic computations on thermal analysis data. Thermochimica acta. 2011;520:1-19.
[13] Akbari V, Najafi F, Vahabi H, Jouyandeh M, Badawi M, Morisset S, et al. Surface chemistry of halloysite nanotubes controls the curability of low filled epoxy nanocomposites. Progress in Organic Coatings. 2019;135:555--64.
[14] Tikhani F, Jouyandeh M, Jafari SH, Chabokrow S, Ghahari M, Gharanjig K, et al. Cure Index demonstrates curing of epoxy composites containing silica nanoparticles of variable morphology and porosity. Progress in Organic Coatings. 2019;135:176-84.
[15] Jouyandeh M, Paran SMR, Jannesari A, Saeb MR. 'Cure Index' for thermoset composites. Progress in Organic Coatings. 2019;127:429-34.
[16] Jouyandeh M, Zarrintaj P, Ganjali MR, Ali JA, Karimzadeh I, Aghazadeh M, et al. Curing epoxy with electrochemically synthesized GdxFe3-xO4 magnetic nanoparticles. Progress in Organic Coatings. 2019;136:105245.
[17] Jouyandeh M, Ali JA, Aghazadeh M, Formela K, Saeb MR, Ranjbar Z, et al. Curing epoxy with electrochemically synthesized ZnxFe3-xO4 magnetic nanoparticles. Progress in Organic Coatings. 2019:105246.
[18] Jouyandeh M, Ali JA, Akbari V, Aghazadeh M, Paran SMR, Naderi G, et al. Curing epoxy with polyvinylpyrrolidone (PVP) surface-functionalized MnxFe3-xO4 magnetic nanoparticles. Progress in Organic Coatings. 2019:105247.
[19] Jouyandeh M, Ganjali MR, Ali JA, Aghazadeh M, Paran SMR, Naderi G, et al. Curing epoxy with polyvinylpyrrolidone (PVP) surface-functionalized ZnxFe3-xO4 magnetic nanoparticles. Progress in Organic Coatings. 2019:105227.
[20] Jouyandeh M, Ali JA, Akbari V, Aghazadeh M, Paran SMR, Naderi G, et al. Curing epoxy with polyvinylpyrrolidone (PVP) surface-functionalized MnxFe3-xO4 magnetic nanoparticles. Progress in Organic Coatings. 2019;136:105247.
[21] Farrusseng D. Metal-organic frameworks: applications from catalysis to gas storage: John Wiley & Sons; 2011.
[22] Yang SJ, Kim T, Im JH, Kim YS, Lee K, Jung H, et al. MOF-derived hierarchically porous carbon with exceptional porosity and hydrogen storage capacity. Chemistry of Materials. 2012;24:464-70.
[23] Song Q, Nataraj S, Roussenova MV, Tan JC, Hughes DJ, Li W, et al. Zeolitic imidazolate framework (ZIF-8) based polymer nanocomposite membranes for gas separation. Energy & Environmental Science. 2012;5:8359-69.
[24] Caro J. Are MOF membranes better in gas separation than those made of zeolites? Current Opinion in Chemical Engineering. 2011;1:77-83.

[25] Müller M, Hermes S, Kähler K, van den Berg MW, Muhler M, Fischer RA. Loading of MOF-5 with Cu and ZnO nanoparticles by gas-phase infiltration with organometallic precursors: properties of Cu/ZnO@ MOF-5 as catalyst for methanol synthesis. Chemistry of materials. 2008;20:4576-87.
[26] Xu GW, Wu YP, Dong WW, Zhao J, Wu XQ, Li DS, et al. A multifunctional Tb-MOF for highly discriminative sensing of Eu3+/Dy3+ and as a catalyst support of Ag nanoparticles. Small. 2017;13:1602996.
[27] Horcajada P, Gref R, Baati T, Allan PK, Maurin G, Couvreur P, et al. Metal–organic frameworks in biomedicine. Chemical reviews. 2011;112:1232-68.
[28] Chen W, Wu C. Synthesis, functionalization, and applications of metal–organic frameworks in biomedicine. Dalton Transactions. 2018;47:2114-33.
[29] Rowsell JL, Yaghi OM. Metal–organic frameworks: a new class of porous materials. Microporous and mesoporous materials. 2004;73:3-14.
[30] Xiu-Liang Lv KW, Bin Wang, Jie Su, Xiaodong Zou, Yabo Xie, Jian-Rong Li, and Hong-Cai Zhou. A Base-Resistant Metalloporphyrin MOF for C–H Bond Halogenation. Journal of the American Chemical Society. 2016.
[31] Yang F, Xu G, Dou Y, Wang B, Zhang H, Wu H, et al. A flexible metal–organic framework with a high density of sulfonic acid sites for proton conduction. Nature Energy. 2017;2:877-83.
[32] Yuan S, Feng L, Wang K, Pang J, Bosch M, Lollar C, et al. Stable Metal-Organic Frameworks: Design, Synthesis, and Applications. Adv Mater. 2018;30:e1704303.
[33] Kitagawa S, Kitaura R, Noro Si. Functional porous coordination polymers. Angewandte Chemie International Edition. 2004;43:2334-75.
[34] Rosseinsky M. Recent developments in metal-organic framework chemistry: design, discovery, permanent porosity and flexibility. Microporous and Mesoporous Materials. 2004;1:15-30.
[35] Anbia M, Hoseini V. Enhancement of CO2 adsorption on nanoporous chromium terephthalate (MIL-101) by amine modification. Journal of Natural Gas Chemistry. 2012;21:339-43.
[36] Henschel A, Gedrich K, Kraehnert R, Kaskel S. Catalytic properties of MIL-101. Chem Commun (Camb). 2008:4192-4.
[37] G. Fe´rey CM-D, C. Serre, F. Millange, J. Dutour, S. Surble´, I. Margiolaki. A Chromium Terephthalate–Based Solid with Unusually Large Pore Volumes and Surface Area. SCIENCE. 2005;309:2040-2.
[38] Stock N, Biswas S. Synthesis of metal-organic frameworks (MOFs): routes to various MOF topologies, morphologies, and composites. Chem Rev. 2012;112:933-69.
[39] Qian J, Sun F, Qin L. Hydrothermal synthesis of zeolitic imidazolate framework-67 (ZIF-67) nanocrystals. Materials Letters. 2012;82:220-3.
[40] Zimpel A, Preiß T, Röder R, Engelke H, Ingrisch M, Peller M, et al. Imparting Functionality to MOF Nanoparticles by External Surface Selective Covalent Attachment of Polymers. Chemistry of Materials. 2016;28:3318-26.
[41] Mahdi E, Tan J-C. Mixed-matrix membranes of zeolitic imidazolate framework (ZIF-8)/Matrimid nanocomposite: Thermo-mechanical stability and viscoelasticity underpinning membrane separation performance. Journal of membrane science. 2016;498:276-90.
[42] Hu C, Xiao J-D, Mao X-D, Song L-L, Yang X-Y, Liu S-J. Toughening mechanisms of epoxy resin using aminated metal-organic framework as additive. Materials Letters. 2019;240:113-6.
[43] Srivastava M, Roy P, Ramanan A. Toughening of epoxy resin using Zn4O (1,4-benzenedicarboxylate)3 metal organic framework. RSC Adv. 2014;4.
[44] Manju M, Roy PK, Ramanan A. Toughening of epoxy resin using Zn4O (1,4-benzenedicarboxylate)3 metal–organic frameworks. RSC Adv. 2014;4:52338-45.

[45] Hou Y, Hu W, Gui Z, Hu Y. A novel Co(Ⅱ)–based metal-organic framework with phosphorus-containing structure: Build for enhancing fire safety of epoxy. Composites Science and Technology. 2017;152:231-42.
[46] Wang N, Zhang Y, Chen J, Zhang J, Fang Q. Dopamine modified metal-organic frameworks on anti-corrosion properties of waterborne epoxy coatings. Progress in Organic Coatings. 2017;109:126-34.
[47] Bromberg L, Diao Y, Wu H, Speakman SA, Hatton TA. Chromium(III) Terephthalate Metal Organic Framework (MIL-101): HF-Free Synthesis, Structure, Polyoxometalate Composites, and Catalytic Properties. Chemistry of Materials. 2012;24:1664-75.
[48] Bernt S, Guillerm V, Serre C, Stock N. Direct covalent post-synthetic chemical modification of Cr-MIL-101 using nitrating acid. Chem Commun (Camb). 2011;47:2838-40.
[49] Jhung SH, Lee JH, Yoon JW, Serre C, Férey G, Chang JS. Microwave Synthesis of Chromium Terephthalate MIL-101 and Its Benzene Sorption Ability. Advanced Materials. 2007;19:121-4.
[50] Vu TA, Le GH, Dao CD, Dang LQ, Nguyen KT, Dang PT, et al. Isomorphous substitution of Cr by Fe in MIL-101 framework and its application as a novel heterogeneous photo-Fenton catalyst for reactive dye degradation. RSC Adv. 2014;4:41185-94.
[51] Fang Y, Zhao G, Dai W, Ma L, Ma N. Enhanced adsorption of rubidium ion by a phenol@MIL-101(Cr) composite material. Microporous and Mesoporous Materials. 2017;251:51-7.
[52] Gao L, Li C-YV, Chan K-Y. Polystyrenesulfonate Threaded in MIL-101Cr(III): A Cationic Polyelectrolyte Synthesized Directly into a Metal–Organic Framework. Chemistry of Materials. 2015;27:3601-8.
[53] Kayal S, Sun B, Chakraborty A. Study of metal-organic framework MIL-101(Cr) for natural gas (methane) storage and compare with other MOFs (metal-organic frameworks). Energy. 2015;91:772-81.
[54] Hong DY, Hwang YK, Serre C, Frey G, Chang JS. Porous chromium terephthalate MIL-101 with coordinatively unsaturated sites: Surface functionalization, encapsulation, sorption and catalysis. Advanced Functional Materials. 2009;19:1537--52.
[55] Loiseau T, Férey G. Crystalline oxyfluorinated open-framework compounds: Silicates, metal phosphates, metal fluorides and metal-organic frameworks (MOF). Journal of Fluorine Chemistry. 2007;128:413-22.
[56] Yang J, Zhao Q, Li J, Dong J. Synthesis of metal–organic framework MIL-101 in TMAOH-Cr(NO3)3-H2BDC-H2O and its hydrogen-storage behavior. Microporous and Mesoporous Materials. 2010;130:174-9.
[57] Jouyandeh M, Ganjali MR, Ali JA, Aghazadeh M, Saeb MR, Ray SS. Curing epoxy with polyvinylpyrrolidone (PVP) surface-functionalized NixFe3-xO4 magnetic nanoparticles. Progress in Organic Coatings. 2019:105259.
[58] Ghiyasi S, Sari MG, Shabanian M, Hajibeygi M, Zarrintaj P, Rallini M, et al. Hyperbranched poly(ethyleneimine) physically attached to silica nanoparticles to facilitate curing of epoxy nanocomposite coatings. Progress in Organic Coatings. 2018;120:100--9.
[59] Jouyandeh M, Shabanian M, Khaleghi M, Paran SMR, Ghiyasi S, Vahabi H, et al. Acid-aided epoxy-amine curing reaction as reflected in epoxy/Fe3O4 nanocomposites: Chemistry, mechanism, and fracture behavior. Progress in Organic Coatings. 2018;125:384-92.
[60] Jouyandeh M, Paran SMR, Shabanian M, Ghiyasi S, Vahabi H, Badawi M, et al. Curing behavior of epoxy/Fe3O4 nanocomposites: A comparison between the effects of bare Fe3O4, Fe3O4/SiO2/chitosan and Fe3O4/SiO2/chitosan/imide/phenylalanine-modified nanofillers. Progress in Organic Coatings. 2018;123:10-9.
[61] Jouyandeh M, Jazani O, Navarchian A, Saeb M. Epoxy coatings physically cured with hydroxyl-contained silica nanospheres and halloysite nanotubes, progress in color. Colorants Coat. 2018;11:199-207.
[62] Karami Z, Jouyandeh M, Hamad SM, Ganjali MR, Aghazadeh M, Torre L, et al. Curing epoxy with Mg-Al LDH nanoplatelets intercalated with carbonate ion. Progress in Organic Coatings. 2019;136:105278.

[63] Jouyandeh M, Karami Z, Hamad SM, Ganjali MR, Akbari V, Vahabi H, et al. Nonisothermal cure kinetics of epoxy/ZnxFe3-xO4 nanocomposites. Progress in Organic Coatings. 2019;136:105290.
[64] Roy PK, Ramanan A. Toughening of epoxy resin using Zn 4 O (1, 4-benzenedicarboxylate) 3 metal–organic frameworks. RSC Advances. 2014;4:52338-45.
[65] Chen C, Zhang M, Guan Q, Li W. Kinetic and thermodynamic studies on the adsorption of xylenol orange onto MIL-101(Cr). Chemical Engineering Journal. 2012;183:60-7.
[66] Munusamy K, Sethia G, Patil DV, Somayajulu Rallapalli PB, Somani RS, Bajaj HC. Sorption of carbon dioxide, methane, nitrogen and carbon monoxide on MIL-101(Cr): Volumetric measurements and dynamic adsorption studies. Chemical Engineering Journal. 2012;195-196:359-68.
[67] Saeb MR, Najafi F, Bakhshandeh E, Khonakdar HA, Mostafaiyan M, Simon F, et al. Highly curable epoxy/MWCNTs nanocomposites: An effective approach to functionalization of carbon nanotubes. Chemical Engineering Journal. 2015;259:117-25.
[68] Henschel A, Gedrich K, Kraehnert R, Kaskel S. Catalytic properties of MIL-101. Chemical Communications. 2008:4192--4.
[69] Saeb MR, Vahabi H, Jouyandeh M, Movahedifar E, Khalili R. Epoxy-based Flame Retardant Nanocomposite Coatings: Comparison Between Functions of Expandable Graphite and Halloysite Nanotubes. Progress in Color, Colorants and Coatings. 2017;10:245-52.